2013 IEEE 10th International Symposium on Biomedical Imaging:
From Nano to Macro
San Francisco, CA, USA, April 7-11, 2013

ITERATIVE FBP FOR IMPROVED RECONSTRUCTION OF X-RAY DIFFERENTIAL PHASE-CONTRAST TOMOGRAMS

Masih Nilchian[*], *Cédric Vonesch*[*], *Peter Modregger*[§,‡], *Marco Stampanoni*[§,†], *and Michael Unser*[*]

[*]Biomedical Imaging Group, EPFL, Switzerland
[§]Swiss Light Source Paul Scherrer Institute, 5232 Villigen, Switzerland
[†]Institute for Biomedical Engineering, UZH/ETH Zurich, 8092 Zurich, Switzerland
[‡]School of Biology and Medicine, University of Lausanne, 1015 Lausanne, Switzerland

ABSTRACT

X-ray differential phase-contrast tomography is a recently-developed modality for the imaging of low-contrast biological samples. Its mathematical model is based on the first derivative of the Radon transform and the images, in practice, are reconstructed using a variant of filtered back-projection (FBP). In this paper, we develop an alternative reconstruction algorithm with the aim of reducing the number of required views, while maintaining image quality. To that end, we discretize the forward model based on polynomial B-spline functions. Then, we formulate the reconstruction as a regularized weighted-norm optimization problem with a penalty on the total variation (TV) of the solution. This leads to the derivation of a novel iterative algorithm that involves an alternation of gradient updates (FBP step) and shrinkage-thresholding (within the framework of the fast iterative shrinkage-thresholding algorithm). Experiments with real data suggest that the proposed method significantly improves upon FBP; it can handle a drastic reduction in the number of projections without noticeable degradation of the quality with respect to the standard procedure.

Index Terms— Differential phase-contrast imaging, Iterative filtered back-projection, B-spline functions, Total-variation regularization.

1. INTRODUCTION

X-ray phase-contrast imaging modalities are promising alternatives to conventional tomography for visualizing the structure of many biological samples. Phase-contrast methods can be divided into analyzer-based [1], interferometric [2], and propagation-based techniques [3]. The differences between these methods are related to their physical setup and the signal that they measure.

The physical setup of X-ray differential phase-contrast imaging (DPCI) is based on grating interferometry [4]. Its physical model involves the first derivative of the object's refractive-index. The consequence is that images can be reconstructed using a variant of the filtered back-projection (FBP) algorithm found with conventional tomography. Because the FBP method requires a large number of view angles, the total scan time can be very long. Our main goal in this work is to reduce the number of views, hence the total acquisition time, while maintaining image quality. This is made possible through the refinement of the reconstruction procedure and the introduction of regularization constraints.

The development of iterative methods for DPCI is very recent [5–8]. Their common philosophy is a maximum-a-posteriori type criterion which involves a least-squares data term and a suitable regularization term. In this paper, we investigate an alternative approach for deriving an iterative algorithm with good convergence properties. The key idea is to take advantage of the FBP in the course of iteration. It is a concept that originates from CT [9], but which has not yet been transposed to DPCI. The contributions of this paper are

- A rigorous discretization of the DPCI forward model using B-splines.
- A variational formulation of iterative FBP involving a weighted-norm least-squares term with a penalty that imposes a regularization on the solution.
- A fast iterative-shrinkage algorithm tailored to the problem.
- The demonstration on real data that the approach can significantly reduce the acquisition time at no cost in image quality.

The paper is organized as follows: We describe the physical model of DPCI followed by our discretization scheme and the required mathematical properties in Section 2. In Section 3, we present our variational formulation and the resulting reconstruction algorithm. We formulate the reconstruction as a regularized weighted-norm optimization problem and derive our new reconstruction scheme. We present a real experiment to validate the proposed method in Section 4. We summarize and conclude our work in Section 5.

2. FORWARD MODEL

2.1. Physical Model

An X-ray plane wave can be characterized by its intensity and phase. However, only the intensity is directly measurable. Therefore, to access the phase information, it is necessary to transfer it to the intensity domain. To that end, the physical setup of DPCI is based on grating interferometry (GI), as shown in Figure 1. Two grating layers are placed behind the object (with respect to the beam source). The first grating is a phase grating that produces a phase shift of π. The second grating is an absorption grating.

The object, which is illuminated by a plane wave, introduces the phase shift $\triangle\phi(y,\theta)$ in the transmitted wave. Its proportionality to

This work was funded (in part) by ERC Grant ERC-2010-AdG 267439-FUN-SP, the Swiss National Science Foundation under Grant 200020-144355 and the Center for Biomedical Imaging of the Geneva-Lausanne Universities and EPFL.

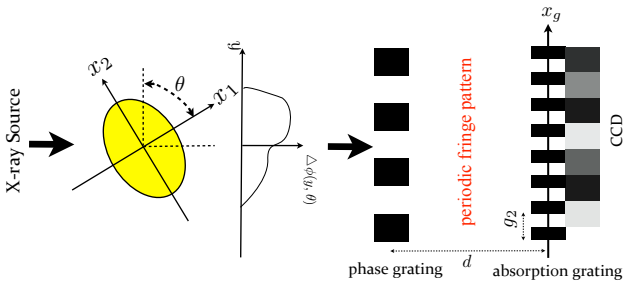

Fig. 1: The physical setup of differential phase-contrast imaging is based on grating interferometers. The phase grating introduces a phase shift in the transmitted wave. The absorption grating is used to adjust the received wave to the resolution of the detector.

the Radon transform of the refractive index is expressed by

$$\triangle\phi(y,\theta) = \frac{2\pi}{\lambda}\mathcal{R}\{f(x_1,x_2)\}(y,\theta)\,,$$

where

$$\mathcal{R}\{f\}(y,\theta) = \int_{\mathbb{R}^2} f(\boldsymbol{x})\delta(y-\langle\boldsymbol{x},\boldsymbol{\theta}\rangle)\mathrm{d}\boldsymbol{x}\,,$$

with $\boldsymbol{x} = (x_1, x_2)$ and $\boldsymbol{\theta} = (\cos\theta, \sin\theta)$. The Radon transform $\mathcal{R}\{f\}(y,\theta)$, with $y \in \mathbb{R}$ and $\theta \in [0,\pi]$, represents the set of line integrals of $f \in L_2(\mathbb{R}^2)$ perpendicular to $\boldsymbol{\theta}$ with (signed) distance y from the origin.

The object causes the wave to be refracted; the refraction angle is proportional to the derivative of the phase shift with respect to y. The wave then reaches the phase grating which essentially splits it into first and second diffraction orders. Since the period of the grating ($4\mu m$) is much larger than the wavelength, the angle between the two diffracted beams is very small and they overlap almost completely. When there is no object, the illumination plane wave produces a periodic fringe pattern at the detector with a period that is half the grating pitch.

The changes in the refraction angle induced by the object lead to some local displacements of the fringes at the detector. An absorption grating is placed at distance d and a phase stepping technique (PST) [4] is used to extract the pulse shifts at each pixel. The latter is proportional to the refraction angle induced by the object. Therefore, the physical model of DPCI is based on the first derivative of the Radon transform (FDRT) of the refractive index of the object f;

$$g(y,\theta) = \frac{g_2}{2\pi d}\phi(y,\theta) = \frac{\partial}{\partial y}\mathcal{R}\{f\}(y,\theta)\,, \tag{1}$$

where $\phi(y,\theta)$ is the phase of the intensity oscillation at each pixel, and g_2 is the absorption grating period.

2.2. Model Discretization

To formulate the reconstruction problem, it is necessary to discretize the forward imaging operator. We use the discretization scheme based on polynomial B-spline functions proposed in [7]. This leads to the matrix version of (1) given by

$$\mathbf{g} = \mathbf{H}\mathbf{c}, \tag{2}$$

where $\mathbf{c}$ is a vector of B-spline coefficients in lexical order, $\mathbf{g}$ is the output vector, and $\mathbf{H}$ is the system matrix with

$$[\mathbf{H}]_{(i,j),\boldsymbol{k}} = \mathcal{R}^{(1)}\{\beta^n(\cdot-\boldsymbol{k})\}(y_j,\theta_i)\,, \tag{3}$$

and $\theta_i = i \triangle \theta$ and $y_j = j \triangle y$. We use tensor-product B-splines of degree n: $\beta^n(\boldsymbol{x}) = \beta^n(x_1)\beta^n(x_2)$. The B-spline is $\beta^n(x) = \frac{\triangle_1^{n+1}}{n!}x_+^n$, where $\triangle_h^n f(x)$ is the n-fold iteration of the finite-difference operator $\triangle_h f(x) = \frac{f(x+h/2)-f(x-h/2)}{h}$ and $x_+ = \max(0,x)$. Therefore, to compute the matrix entries, it is sufficient to have $\mathcal{R}^{(1)}\beta^n(y_j,\theta_i)$, with

$$\mathcal{R}^{(1)}\{\beta^n\}(y,\theta) = \frac{\triangle_{\cos\theta}^{n+1}\triangle_{\sin\theta}^{n+1}}{(2n)!}y_+^{2n}\,.$$

2.3. Modified FBP for DPCI

Since the data is a derivative of the Radon transform, one can use a variant of FBP. For brevity, let us denote the FDRT of f by,

$$\mathcal{R}^{(1)}f(y,\theta) = \frac{\partial}{\partial y}\mathcal{R}f(y,\theta)\,.$$

Proposition 1. [Modified filtered back-projection]

$$\mathcal{R}^{(1)^*}\{h(\cdot) * \mathcal{R}^{(1)}f(\cdot,\theta)\}(\boldsymbol{x}) = f(\boldsymbol{x})\,, \tag{4}$$

where $\mathcal{R}^{(1)^*}$ is the adjoint of the first derivative of the Radon transform operator and h is the convolution kernel whose Fourier transform is $\widehat{h}(\omega) = \frac{1}{|\omega|}$.

Proof. Since the adjoint of $\frac{\partial}{\partial y}$ is $-\frac{\partial}{\partial y}$, we have

$$\begin{aligned}\mathcal{R}^{(1)^*}\{\mathcal{R}^{(1)}f\}(\boldsymbol{x}) &= -\mathcal{R}^*\{\frac{\partial^2}{\partial y^2}\mathcal{R}f(y,\cdot)\}(\boldsymbol{x})\\ &\overset{(A)}{=} (-\triangle)\{\mathcal{R}^*\{\mathcal{R}f\}\}(\boldsymbol{x})\\ &\overset{(B)}{=} (-\triangle)^{\frac{1}{2}}\{f\}(\boldsymbol{x})\end{aligned}$$

where $\mathcal{R}^*$ is the Radon adjoint operator defined as

$$\mathcal{R}^*\{g\}(\boldsymbol{x}) = \int_0^\pi g(\langle\boldsymbol{x},\boldsymbol{\theta}\rangle,\theta)\mathrm{d}\theta\,,$$

with $g(y,\theta) \in L_2(\mathbb{R}\times[0,\pi])$. $(-\triangle)$ and $(-\triangle)^{\frac{1}{2}}$ are the Laplace and square-root Laplace operators, whose Fourier transforms are $||\boldsymbol{\omega}||^2$ and $||\boldsymbol{\omega}||$, respectively. The Fourier-slice theorem results in (A). The sequential application of the Radon adjoint and the Radon transform on the function f is the filtering operator

$$\mathcal{R}^*\{\mathcal{R}f\}(\boldsymbol{x}) = 2\pi(-\triangle)^{-\frac{1}{2}}\{f\}(\boldsymbol{x})\,, \tag{5}$$

where $(-\triangle)^{-\frac{1}{2}}$ is a fractional integral operator with transfer function $\frac{1}{||\boldsymbol{\omega}||}$. It yields the equality (B). We thus have

$$(-\triangle)^{-\frac{1}{2}}\mathcal{R}^{(1)^*}\{\mathcal{R}^{(1)}f\}(\boldsymbol{x}) = f(\boldsymbol{x})\,,$$

which implies (4) using the Fourier-slice theorem. □

Within our discretization framework, the modified FBP described by Proposition 1 is expressed as

$$\mathbf{c}_0 = \mathbf{H}^T\mathbf{W}\mathbf{g}\,, \tag{6}$$

where $\mathbf{g}$ is an $(M\times 1)$ data vector, $\mathbf{W}$ corresponds to the filtering operation in (4), $\mathbf{H}$ is the $(M\times N)$ forward projection matrix (3), and $\mathbf{H}^T$ is its transpose. It is the standard technique that is used in practice for the reconstruction of DPCI tomograms.

3. IMAGE RECONSTRUCTION

We shall now see how the quality of the reconstructions can be improved through iterations. The key observation is that (6) corresponds to the first iteration of a basic steepest-descent algorithm on the weighted least-squares criterion

$$\tfrac{1}{2}||\mathbf{Hc}-\mathbf{g}||^2_{\mathbf{W}} = (\mathbf{Hc}-\mathbf{g})^T\mathbf{W}(\mathbf{Hc}-\mathbf{g})\,, \tag{7}$$

which is aimed at imposing consistency between the reconstructed image and the measurements.

In order to derive our algorithm, we make two crucial modifications to this criterion. First, we adjust the frequency response of the theoretical filter in Proposition 1 to avoid the singularity at zero, replacing it with the filter $\tilde{\mathbf{W}}$ whose response is $\frac{1}{|\omega|+\lambda}$, which has also the advantage of being positive-definite. Second, we handle the fact that the reconstruction problem is ill-posed (in the case of a limited number of views) by adding a suitable regularization term.

We therefore reformulate the reconstruction in terms of the optimization problem

$$\underset{\mathbf{c}}{\operatorname{argmin}}\{J(\mathbf{c}) \triangleq \tfrac{1}{2}||\mathbf{Hc}-\mathbf{g}||^2_{\tilde{\mathbf{W}}} + \Psi(\mathbf{c})\}\,, \tag{8}$$

where $\Psi(\mathbf{c})$ is the regularization term.

We use total-variation (TV) regularization to enhance edges in the reconstructed image. Since the null space of the imaging operator contains a zero frequency, we also use Tikhonov regularization,

$$\underset{\mathbf{c}}{\operatorname{argmin}}\{J(\mathbf{c}) = \underbrace{\tfrac{1}{2}||\mathbf{Hc}-\mathbf{g}||^2_{\tilde{\mathbf{W}}} + \lambda_1||\mathbf{c}||^2}_{J_1(\mathbf{c})} + \lambda_2\underbrace{\sum_i ||\{\mathbf{Lc}\}_i||_1}_{J_2(\mathbf{c})}\}\,, \tag{9}$$

where the sum is computed over every B-spline coefficient and $\{\mathbf{Lc}\}_i \in \mathbb{R}^2$ is the gradient vector of the image at position i. The discrete gradient operator is computed using Proposition 2.

Proposition 2. *Let $f(\boldsymbol{x}) = \sum_{\boldsymbol{k}} c_{\boldsymbol{k}}\beta^n(\boldsymbol{x}-\boldsymbol{k})$. The gradient of f on the Cartesian grid is*

$$\begin{aligned}\frac{\partial f}{\partial x_1}[k_1,k_2] &= ((h_1[\cdot,k_2]*c[\cdot,k_2])[k1,\cdot]*b_2[k_1,\cdot])[k_1,k_2]\\ \frac{\partial f}{\partial x_2}[k_1,k_2] &= ((h_2[k_1,\cdot]*c[k_1,\cdot])[\cdot,k_2]*b_1[\cdot,k_2])[k_1,k_2]\,,\end{aligned} \tag{10}$$

where $k_1,k_2\in\mathbb{Z}$, $h_i[k_1,k_2] = \beta^{n-1}(k_i+\frac{1}{2}) - \beta^{n-1}(k_i-\frac{1}{2})$, and $b_i[k_1,k_2] = \beta^n(k_i)$ for $i=1,2$.

To solve the nonlinear TV problem, we develop a modified version of the gradient-based fast iterative shrinkage-thresholding algorithm (FISTA) method [10], which requires the repeated evaluation of the proximal map of the non-smooth part, $J_2(\mathbf{c})$. It is given by

$$\operatorname{prox}_\lambda\{J_2\}(\mathbf{z}) = \underset{\boldsymbol{u}}{\operatorname{argmin}}\left\{\frac{1}{2}||\mathbf{z}-\boldsymbol{u}||^2 + \lambda\sum_i||\{\mathbf{L}\boldsymbol{u}\}_i||_1\right\}. \tag{11}$$

To find the solution of (11), we express the second term in the dual space using a dual ball $\mathcal{B}_{(\mathbf{p},\mathbf{q})}$ and the corresponding dual variable pair $(\mathbf{p},\mathbf{q})$,

$$\sum_i||\{\mathbf{L}\boldsymbol{u}\}_i||_1 = \max_{(\mathbf{p},\mathbf{q})\in\mathcal{B}_{(\mathbf{p},\mathbf{q})}}\left\langle \mathbf{L}^T(\mathbf{p},\mathbf{q}),\boldsymbol{u}\right\rangle,$$

where $\mathbf{L}^T$ is the adjoint of the discrete gradient operator $\mathbf{L}$. We have that

$$\begin{aligned}&\min_{\boldsymbol{u}}\frac{1}{2}||\mathbf{z}-\boldsymbol{u}||^2 + \lambda\sum_i||\{\mathbf{L}\boldsymbol{u}\}_i||_1\\ &= \min_{\boldsymbol{u}}\max_{(\mathbf{p},\mathbf{q})\in\mathcal{B}_{(\mathbf{p},\mathbf{q})}}\frac{1}{2}||\mathbf{z}-\boldsymbol{u}||^2 + \lambda\left\langle\mathbf{L}^T(\mathbf{p},\mathbf{q}),\boldsymbol{u}\right\rangle\\ &= \max_{(\mathbf{p},\mathbf{q})\in\mathcal{B}_{(\mathbf{p},\mathbf{q})}}\frac{1}{2}||\mathbf{z}-\lambda\mathbf{L}^T(\mathbf{p},\mathbf{q})||^2 - \frac{1}{2}||\mathbf{z}||^2\,.\end{aligned}$$

Thus, $\operatorname{prox}_\lambda\{J_2\}(\mathbf{z}) = \mathbf{z}-\lambda\mathbf{L}^T(\mathbf{p}^*,\mathbf{q}^*)$, where

$$(\mathbf{p}^*,\mathbf{q}^*) = \underset{(\mathbf{p},\mathbf{q})}{\operatorname{argmin}}\frac{1}{2}||\mathbf{z}-\lambda\mathbf{L}^T(\mathbf{p},\mathbf{q})||^2 + \mathbf{1}_{\mathcal{B}_{(\mathbf{p},\mathbf{q})}}(\mathbf{p},\mathbf{q})\,. \tag{12}$$

Problem (12) is then solved using the FISTA algorithm. The final ingredient is the gradient of the quadratic function $J_1(\mathbf{c})$

$$\nabla\mathbf{J_1}(\mathbf{c}) = \left(\mathbf{H}^T\tilde{\mathbf{W}}\mathbf{H}+\lambda_1\mathbf{I}\right)\mathbf{c} - \mathbf{H}^T\tilde{\mathbf{W}}\mathbf{g}\,.$$

The resulting reconstruction procedure is summarized in Algorithm 1. Since the condition number of $(\mathbf{H}\tilde{\mathbf{W}}\mathbf{H}+\lambda_1\mathbf{I})$ is close to 1, our iterative FBP can be expected to converge rapidly.

Algorithm 1 FISTA-BASED ITERATIVE FBP

Input: $\mathbf{H}^T\tilde{\mathbf{W}}\mathbf{H}+\lambda_1\mathbf{I}$, $\boldsymbol{\nu} = \mathbf{H}^T\tilde{\mathbf{W}}\mathbf{g}$, $\mathbf{c}_0$, $\tau \le \lambda_{\max}(\mathbf{H}\tilde{\mathbf{W}}\mathbf{H}+\lambda_1\mathbf{I})$, and $\operatorname{prox}_\lambda\{J_2\}$.
Output: The reconstructed image f.

```
Initialization: n = 0, u_0 = c_0, t_0 = 1.
repeat
    c_{n+1} ← prox_{τλ_2}{J_2}(u_n + τ(ν − (H^T W̃ H + λ_1 I)u_n)).
    t_{n+1} ← (1 + sqrt(1 + 4t_n^2))/2.
    u_{n+1} ← c_{n+1} + ((t_n − 1)/t_{n+1})(c_{n+1} − c_n).
    n ← n + 1.
until convergence.
f(x) = Σ_k c_k β^n(x − k).
```

4. EXPERIMENTAL RESULTS

To validate the proposed reconstruction method, we conducted experiments with real data acquired at the TOMCAT beam line of the Swiss Light Source at the Paul Scherrer Institute in Villigen, Switzerland. The synchrotron light is delivered by a 2.9 T super-bending magnet [11]. The energy of the X-ray beam is 25 kev. Each projection contains nine phase steps over two periods to describe the corresponding curve of the PST. For each step, a complete 180-degree tomogram is collected. The projections are collected using a CCD camera to record the individual projections.

We assembled a real phantom composed of a tube with three cylindrical sub regions that are filled with liquids of different refractive indices. A cross section is the 2-D sample that we retain. Its size is 1357×1357 pixels.

We took measurements along 1200 projection angles and used the reconstruction obtained with the FISTA-based iterative FBP method as the ground truth. We then used a subset of the measurements to compare the performance of the traditional FBP algorithm with our method.

We used cubic B-spline for our algorithm. Based on our experience, the Tikhonov regularization parameter can be very small; we

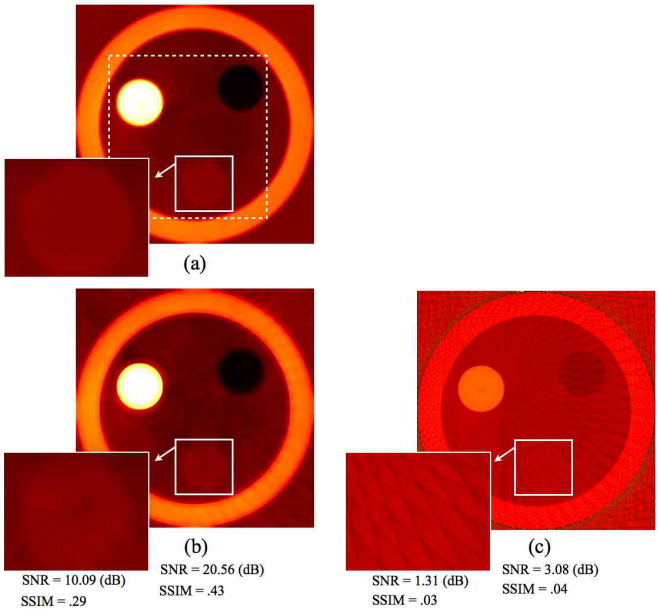

Fig. 2: The reconstructed phantom using FISTA-based iterative FBP method with 1200 directions is considered as the oracle (a). The images reconstructed from 38 projections using our method and an FBP-type method are shown in (b) and (c), respectively.

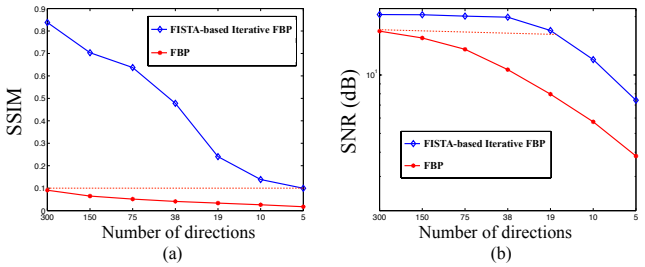

Fig. 3: The SSIM and SNR metrics for images reconstructed from a subset of projections.

set it to 10^{-5}. The TV parameter is set to $10^{-2} \times ||\mathbf{g}||_2$ where $\mathbf{g}$ is the measurement vector.

The reconstructed images using our algorithm and the FBP-like method with 38 projection angles are shown in Figure 2. To compare the reconstructed images, we use the signal-to-noise ratio (SNR) and the structural similarity measure (SSIM [12]) with a window size of 20.

The FBP-like method performs poorly on the boundaries of the image, as exemplified in Figure 2.c. To compare the reconstructions with different numbers of projections, we consider a region in the middle of the object as marked with the white dashed line in Figure 2.a. The comparison results are shown in Figure 3. These results suggest that the proposed algorithm is capable of reconstructing the data as well as the standard imaging procedure, while using only one-twentieth of the number of viewing angles.

5. CONCLUSION

We have formulated a novel iterative FPB algorithm for X-ray differential phase-contrast tomography. The algorithm was derived from the minimization of a weighted-norm error criterion subject to suitable ℓ_1-ℓ_2 regularization constraints. The quality of the physical phantom reconstruction is excellent, including in extreme conditions where the number of views is reduced by a whole order of magnitude.

6. REFERENCES

[1] V.N. Ingal and E.A. Beliaevskaya, "X-ray plane-wave tomography observation of the phase contrast from a non-crystalline object," *J. Phys. D: Appl. Phys*, vol. 28, pp. 2314–2317, 1995.

[2] A. Momose, T. Takeda, Y. itai, and K. Hirano, "Phase-contrast x-ray computed tomography for observing biological soft tissues," *Nat. Med*, vol. 2, pp. 473–475, 1996.

[3] A. Snigirev, I. Snigireva, V. Kohn, S. Kuznetsov, and I. Schelekov, "On the possibilities of X-ray phase-contrast microimaging by coherent high-energy synchroton radiation," *Rev. Sci. Instrum.*, vol. 66, pp. 5486, 1997.

[4] T. Weitkamp, A. Diaz, C. David, F. Pfeiffer, M. Stampanoni, P. Cloetens, E. Ziegler, et al., "X-ray phase imaging with a grating interferometer," *Opt. Express*, vol. 13, no. 16, pp. 6296–6304, 2005.

[5] Z. Qi, J. Zambelli, N. Bevins, and G. Chen, "A novel method to reduce data acquisition time in differential phase contrast computed tomography using compressed sensing," *Proc. of SPIE*, vol. 7258, pp. 4A1–8, 2009.

[6] T. Köhler, B. Brendel, and E. Roessl, "Iterative reconstruction for differential phase contrast imaging using spherically symmetric basis functions," *Medical physics*, vol. 38, pp. 4542, 2011.

[7] M. Nilchian and M. Unser, "Differential phase-contrast X-ray computed tomography: From model discretization to image reconstruction," in *Proceedings of the Ninth IEEE International Symposium on Biomedical Imaging: From Nano to Macro (ISBI'12)*, Barcelona, Spain, May 2-5, 2012, pp. 90–93.

[8] Q. Xu, Emil Y. Sidky, X. Pan, M. Stampanoni, P. Modregger, and M. A. Anastasio, "Investigation of discrete imaging models and iterative image reconstruction in differential X-ray phase-contrast tomography," *Opt. Express*, vol. 20, pp. 10724–10749, 2012.

[9] J. Sunnegardh and P. Danielsson, "Regularized iterative weighted filtered backprojection for helical cone-beam CT," *Medical Physics*, vol. 35, pp. 4173–4185, 2008.

[10] A. Beck and M. Teboulle, "Fast gradient-based algorithms for constrained total variation image denoising and deblurring problems," *IEEE Trans. on image processing*, vol. 18, pp. 2419–2434, 2009.

[11] S.A. McDonald, F. Marone, C. Hintermuller, G. Mikuljan, C. David, F. Pfeiffer, and M. Stampanoni, "Advanced phase-contrast imaging using a grating interferometer," *Synchrotron Radiation*, vol. 16, pp. 562–572, 2009.

[12] Z. Wang and A.C. Bovik, "A universal image quality index," *Signal Processing Letters, IEEE*, vol. 9, no. 3, pp. 81 –84, March 2002.